eLIFE elifesciences.org

RESEARCH ARTICLE

Figures and figure supplements

Interferon-β-induced miR-1 alleviates toxic protein accumulation by controlling autophagy

Camilla Nehammer *et al*

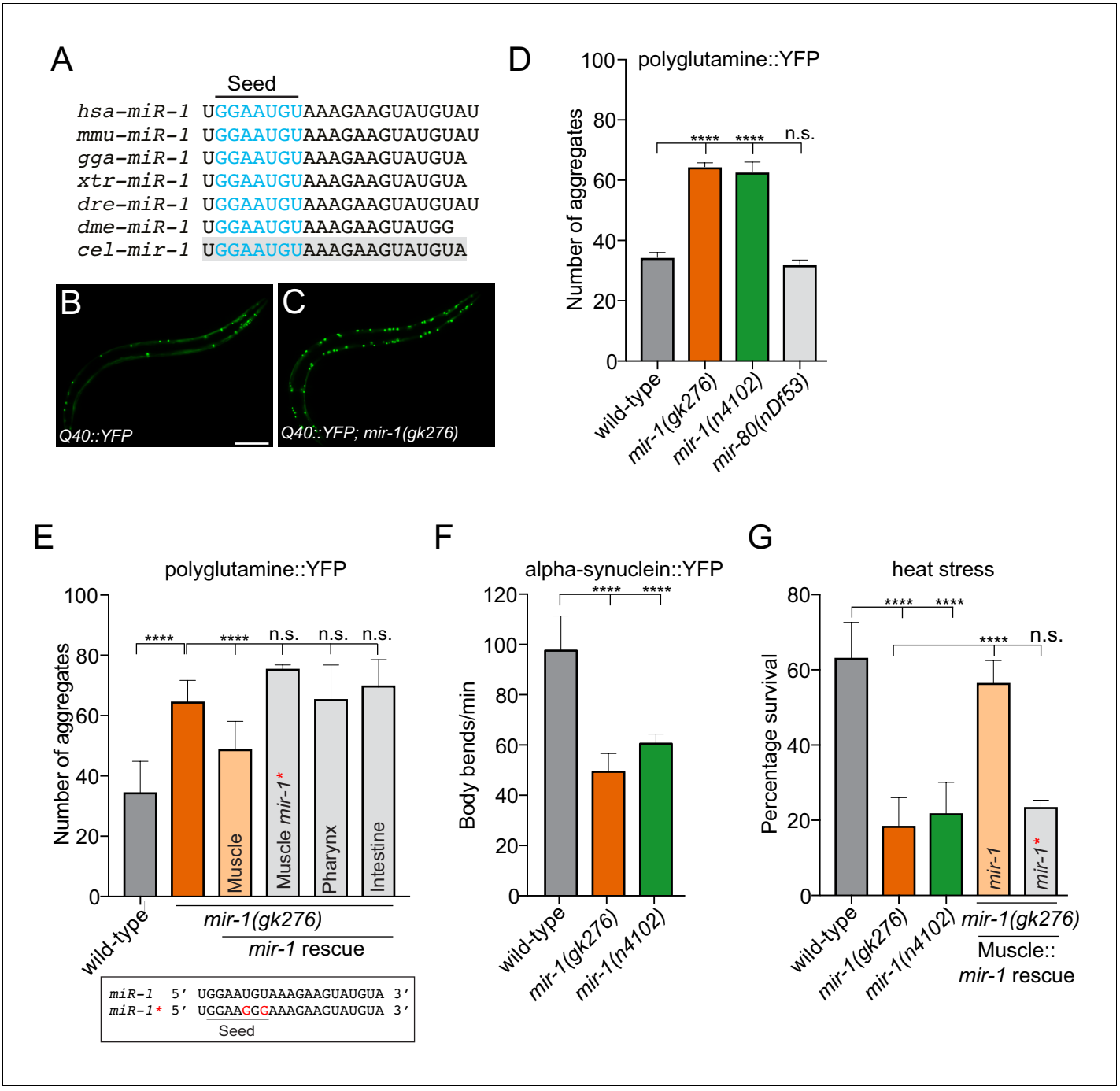

Figure 1. *mir-1* protects against proteotoxic stress. (**A**) Alignment of mature *miR-1* sequences indicates deep conservation. The seed sequence of each *miR-1* family member is highlighted in blue and the conservation of *C. elegans mir-1* is highlighted in gray. *hsa = Homo sapiens, mmu = Mus musculus, gga = Gallus gallus, xtr = Xenopus tropicalis, dre = Danio rerio, dme = Drosophila melanogaster, cel = Caenorhabditis elegans.* (**B–C**) Visualization of Q40::YFP aggregates (green foci) in (**B**) wild-type and (**C**) *mir-1(gk276)* animals. Scale bar, 50 μm. (**D**) Quantification of Q40::YFP aggregation in wild-type, *mir-1(gk276)*, *mir-1(n4102)* and *mir-80(nDf53)* animals. (**E**) Quantification of Q40::YFP aggregates in wild-type, *mir-1(gk276)* and *mir-1(gk276)* animals transgenically-expressing the *mir-1* hairpin in body wall muscle (*myo-3* promoter), pharynx (*myo-2* promoter) or intestine (*ges-1* promoter). Mutation of the *mir-1* seed sequence (Muscle *mir-1**) abrogates rescue from body wall muscle. Mature *mir-1* sequences (wild-type *mir-1* or mutated *mir-1**) used for rescue experiments are shown (box). Red nucleotides indicate the mutations in the seed sequence used in *mir-1** rescue experiments, which are predicted to hinder interactions with *mir-1* targets. (**F**) Body bends in wild-type, *mir-1(gk276)* and *mir-1(n4102)* mutant animals expressing α-synuclein::YFP. (**G**) Survival of wild-type, *mir-1(gk276)* and *mir-1(n4102)* animals after exposure to 4 hr of 35˚C heat stress. Transgenic expression of wild-type *mir-1* hairpin, but not mutated *mir-1**, in body wall muscle rescues *mir-1(gk276)* heat stress sensitivity. All experiments were performed in triplicate

Figure 1 continued on next page

Figure 1 continued

and at least 10 animals were scored per experiment. Error bars show standard error of the mean (SEM). ****p<0.0001, n.s. not significant to the control (one-way ANOVA analysis, followed by Dunnett's multiple comparison test).

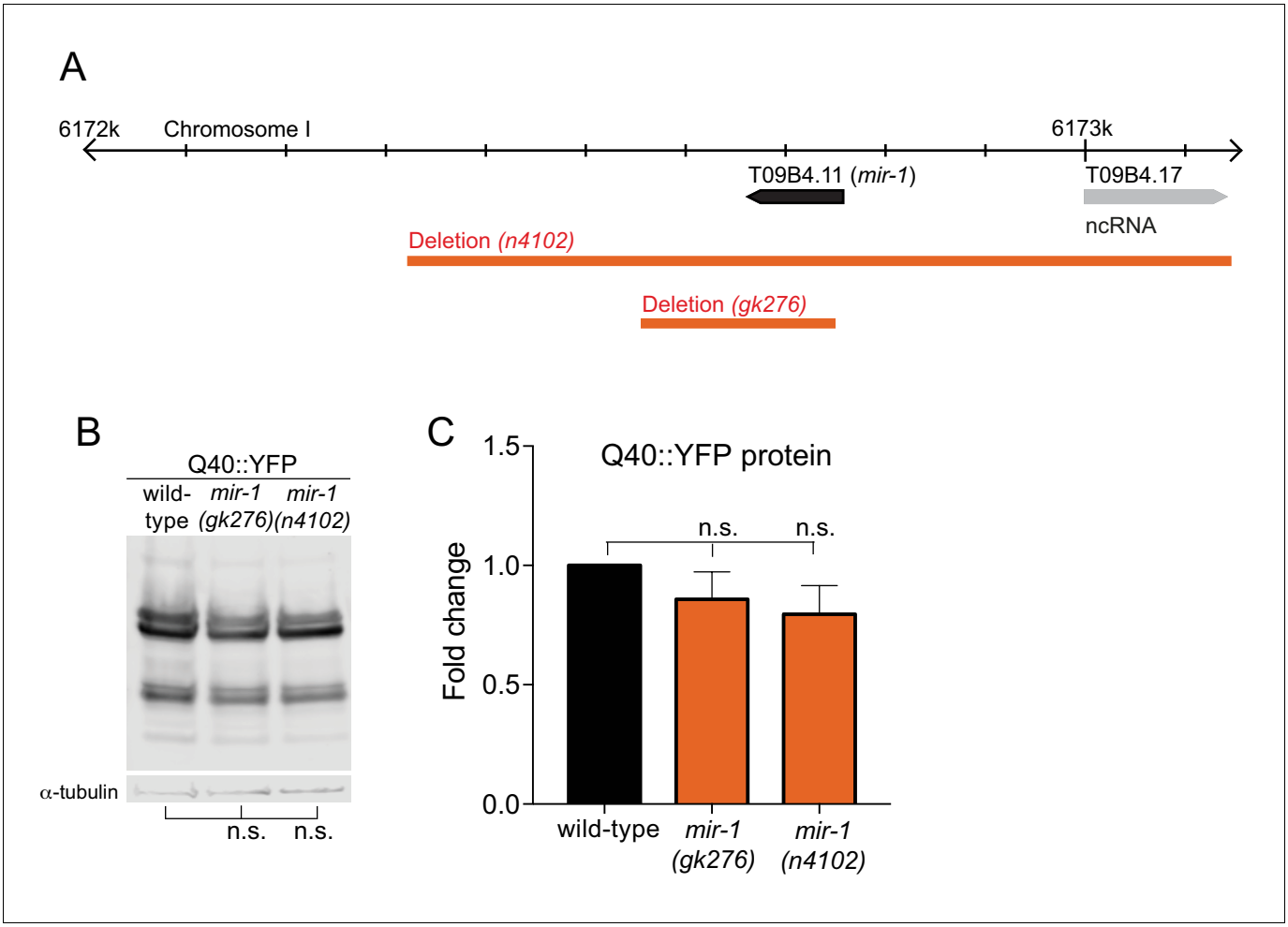

Figure 1—figure supplement 1. Quantification of Q40::YFP Expression. (**A**) Location of *mir-1(T09B4.11)* on chromosome I, reverse strand of assembly; http://www.wormbase.org, WS258, showing the two deletion strains used in this study, *gk276* and *n4102* (orange bars). (**B–C**) WB analysis (**B**) and quantification (**C**) of Q40::YFP protein lysates from wild-type, *mir-1(gk276)* and *mir-1(n4102)* animals for YFP expression using an α-GFP antibody and α-tubulin antibody as a loading control (n = 3). n.s. not significant (one-way ANOVA analysis, followed by Dunnett's multiple comparison test).

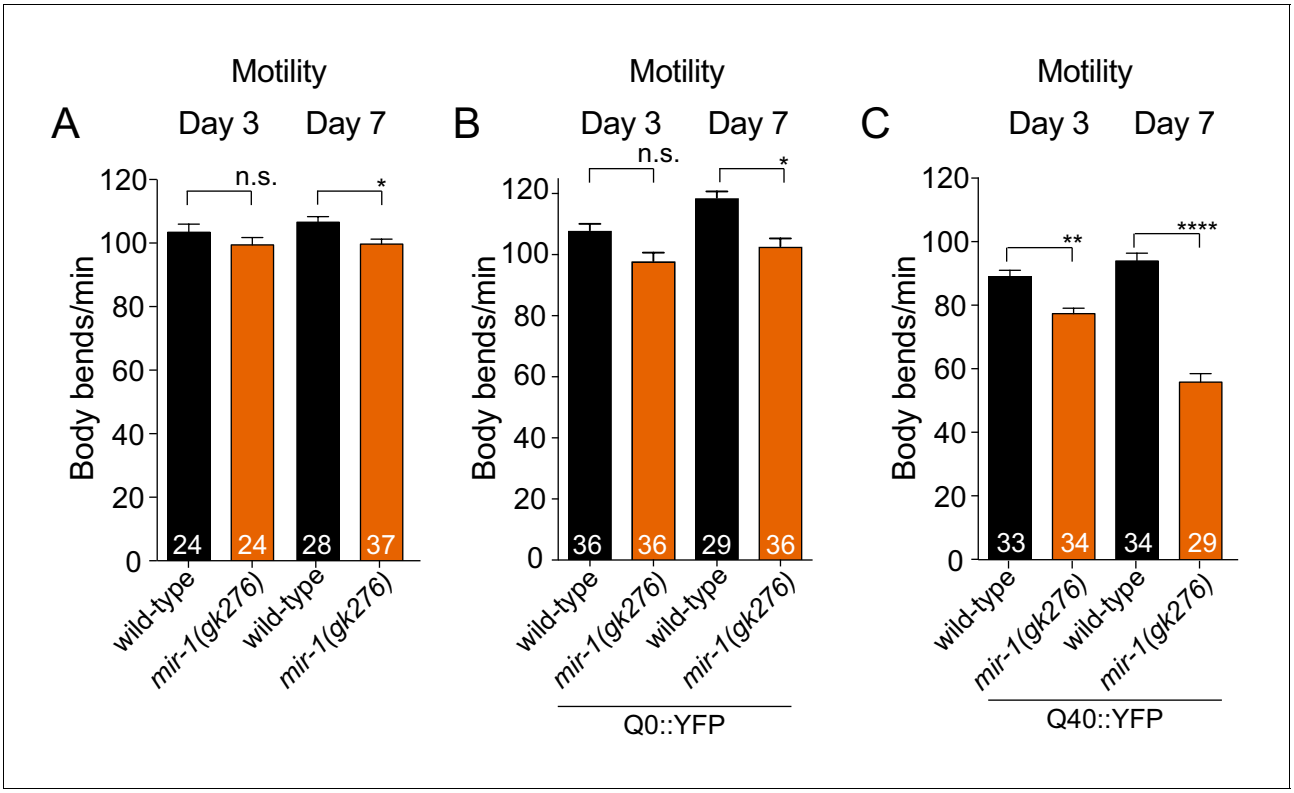

Figure 1—figure supplement 2. Motility Analysis. (**A–C**) Quantification of body bends in wild-type and *mir-1(gk276)* mutant animals without a transgene (**A**), expressing the Q0::YFP transgene (**B**) or expressing the Q40::YFP transgene (**C**). All experiments were performed in triplicate (number of animals scored are shown in each bar). ± SEM. *p<0.05, **p<0.01, ****p<0.0001, n.s. not significant (one-way ANOVA analysis, followed by Dunnett's multiple comparison test).

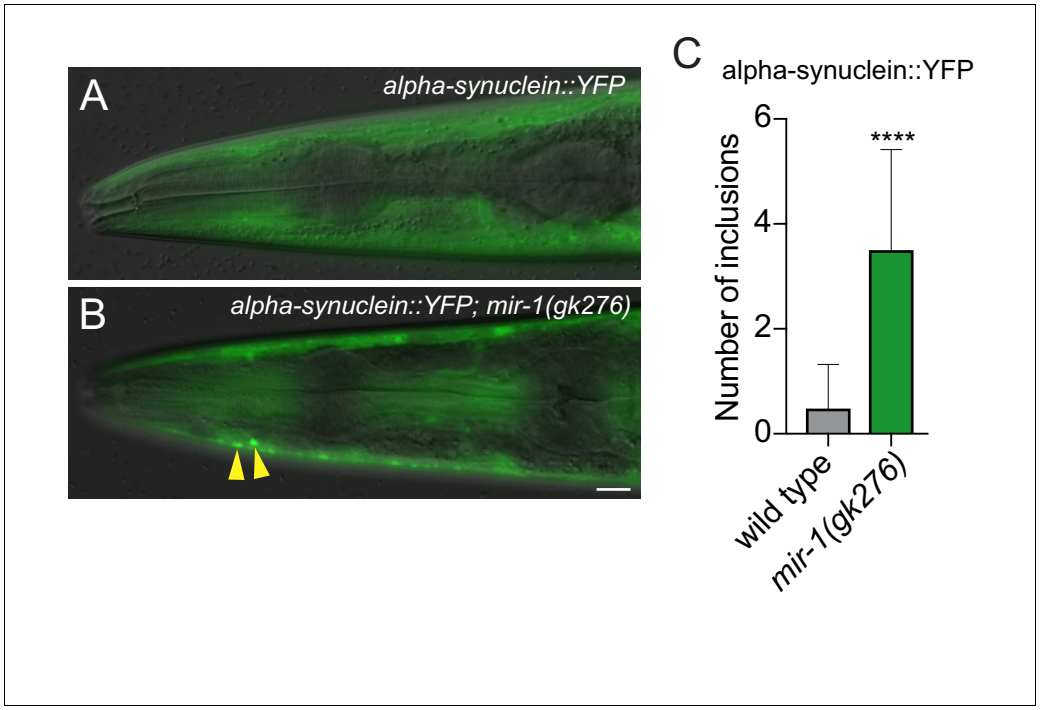

Figure 1—figure supplement 3. *mir-1* prevents the formation of α-synuclein inclusions. (**A–B**) Visualization of α-synuclein::YFP inclusions (yellow arrowheads) in (**A**) wild-type and (**B**) *mir-1(gk276)* animals in the first day of adulthood. Scale bar, 50 µm. (**C**) Quantification of α-synuclein::YFP inclusions in wild-type and *mir-1(gk276)* animals. n > 25. ± SEM ****p<0.0001 (Welch's t-test).

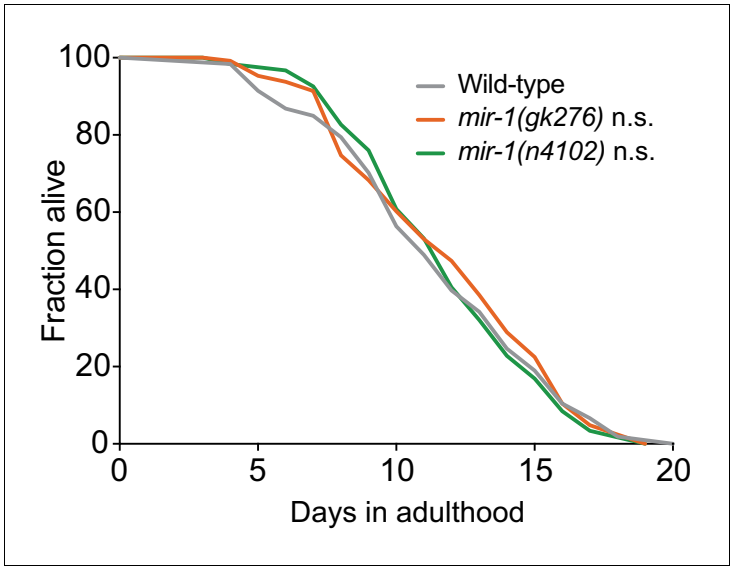

Figure 1—figure supplement 4. *mir-1* Lifespan Analysis. (**A**) Lifespan analysis of wild-type (n = 121), *mir-1(gk276)* (n = 131) and *mir-1(n4102)* (n = 125) animals. Log-rank (Mantel-Cox) test - n.s. not significant.

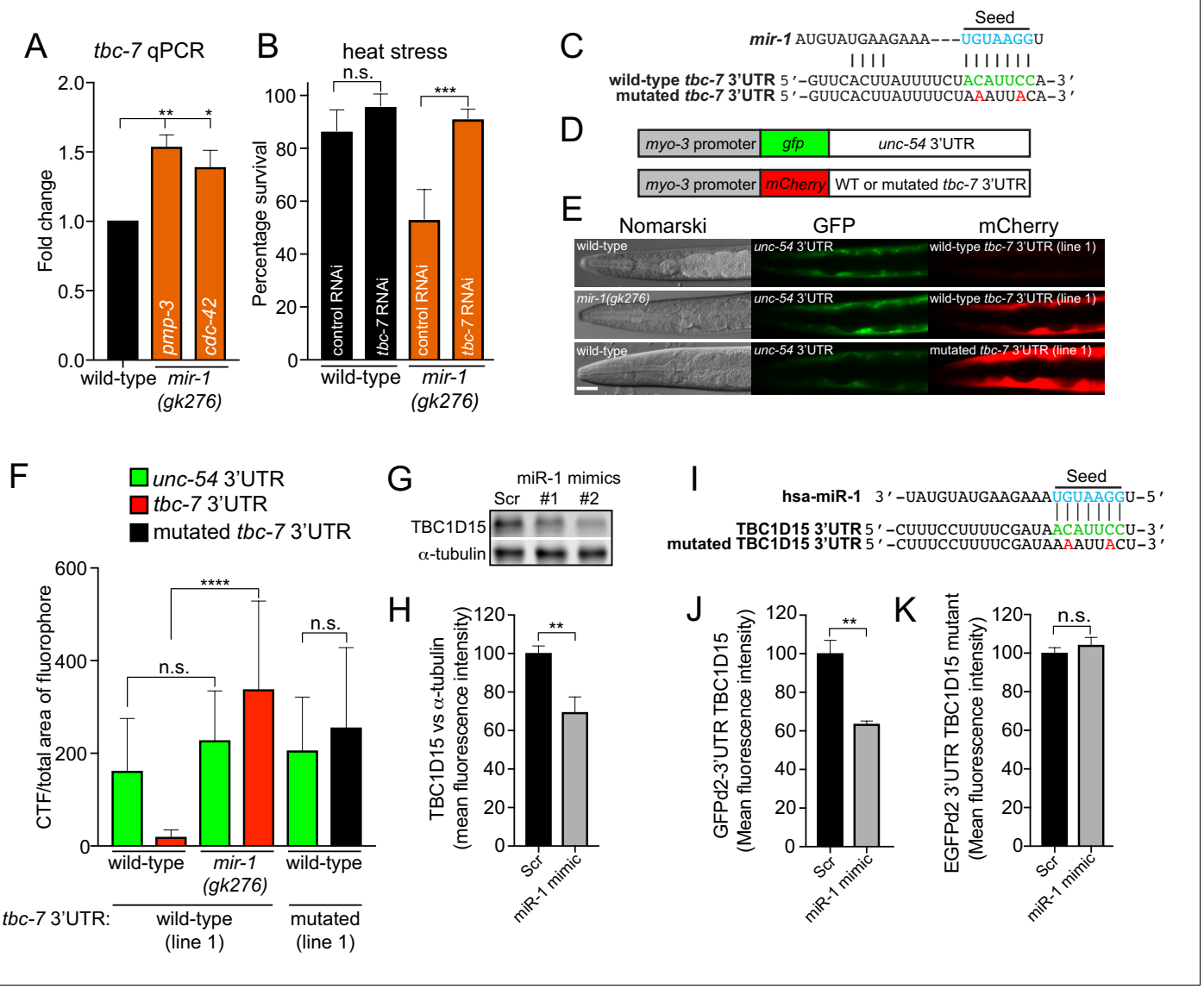

Figure 2. *miR-1* directly regulates TBC 3'UTRs in *C. elegans* and mammals. (**A**) Relative *tbc-7* mRNA levels measured by quantitative real-time PCR in L4 larvae. Data normalized to values for wild-type worms. Two independent reference genes (*pmp-3* and *cdc-42*) were used. Error bars show standard error of the mean (SEM) obtained from n = 3 biological replicates and three technical replicates each. **p<0.001, *p<0.005 (one-way ANOVA analysis, followed by Dunnett's multiple comparison test). (**B**) Survival of wild-type and *mir-1(gk276)* animals (incubated on control (L4440) or *tbc-7* RNAi bacteria) after exposure to 4 hr of heat stress (35˚C) (n = 30). ***p<0.001, n.s. not significant (one-way ANOVA analysis, followed by Dunnett's multiple comparison test). (**C**) Predicted *mir-1* binding site on the 3'UTR of *tbc-7* mRNA (green) and seed sequence in *mir-1* (blue). Mutated nucleotides in the *tbc-7* 3'UTR for experiments (**E–F**) are in red. (**D**) Indicated DNA constructs were co-transformed as multi-copy extrachromosomal arrays for experiments in (**E–F**). (**E**) Expression of heterologous reporter transgenes for control *unc-54* 3'UTR (*gfp*) and wild-type and mutated *tbc-7* 3'UTR (*mCherry*) constructs in body wall muscle. (**F**) Quantification of *gfp* and *mCherry* fluorescence of transgenic animals calculated as CTF/total area of fluorophore (n = 30). ****p<0.0001, n.s. not significant (one-way ANOVA analysis, followed by Dunnett's multiple comparison test). (**G**) WB of TBC1D15 and α-tubulin and (**H**) quantified bands from HeLa cells transfected with scrambled (Scr) or miR-1 mimics (n = 5). Data are mean fluorescence intensities ± SEM. **p<0.01 (Students t-test). (**I**) Predicted miR-1 binding site on the 3'UTR of TBC1D15 mRNA (green) and seed sequence in miR-1 (blue). Mutated nucleotides in the TBC1D15 3'UTR for experiments (**L–M**) are in red. (**J–K**) Quantification of flow cytometry analysis of HeLa cells co-expressing scrambled (Scr) or miR-1 mimic together with (**J**) GFPd2-3'UTR TBC1D15 (n = 4) or (**K**) mutated GFPd2-3'UTR $TBC1D15_{mutant}$ (n = 5). Data are mean fluorescence intensities ± SEM, **p<0.01 (Students t-test).

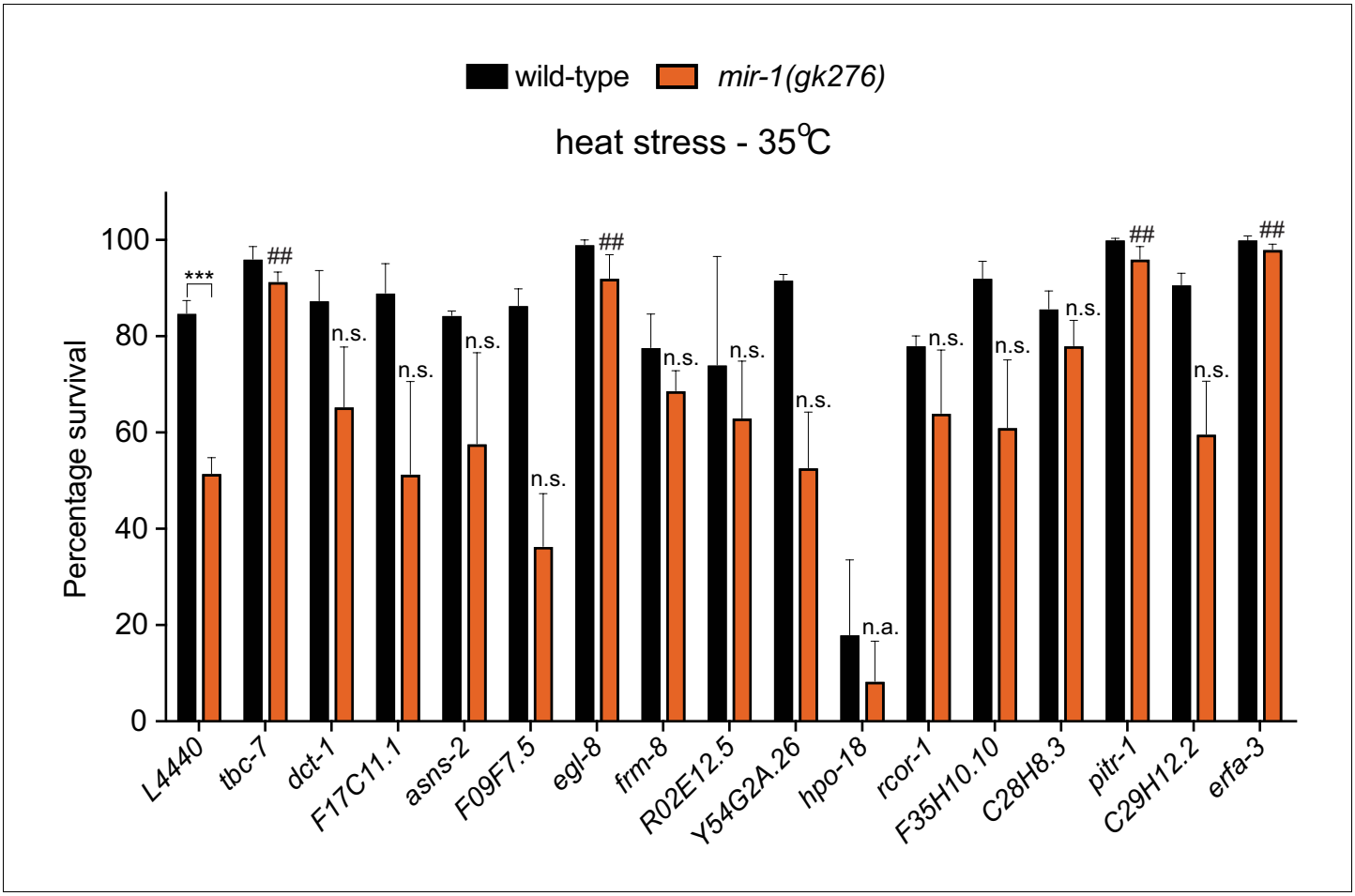

Figure 2—figure supplement 1. RNAi screen to identify *mir-1* targets important for the heat stress response. Survival of wild-type and *mir-1(gk276)* animals after exposure to 4 hr of 35˚C heat stress. Animals were incubated on RNAi bacteria to reduce expression of predicted *mir-1* targets (TargetScanWorm release 6.2). L4440 = control RNAi bacteria. n = 30. ***p<0.001, wild-type compared to *mir-1(gk276)* on control RNAi bacteria. ##p<0.001 and n.s. not significant when comparing knockdown of predicted *mir-1* target to control RNAi in *mir-1(gk276)* animals (one-way ANOVA analysis, followed by Dunnett's multiple comparison test). n.a. - *hpo-18* RNAi causes lethality in wild-type and *mir-1(gk276)* animals. All experiments were performed in triplicate.

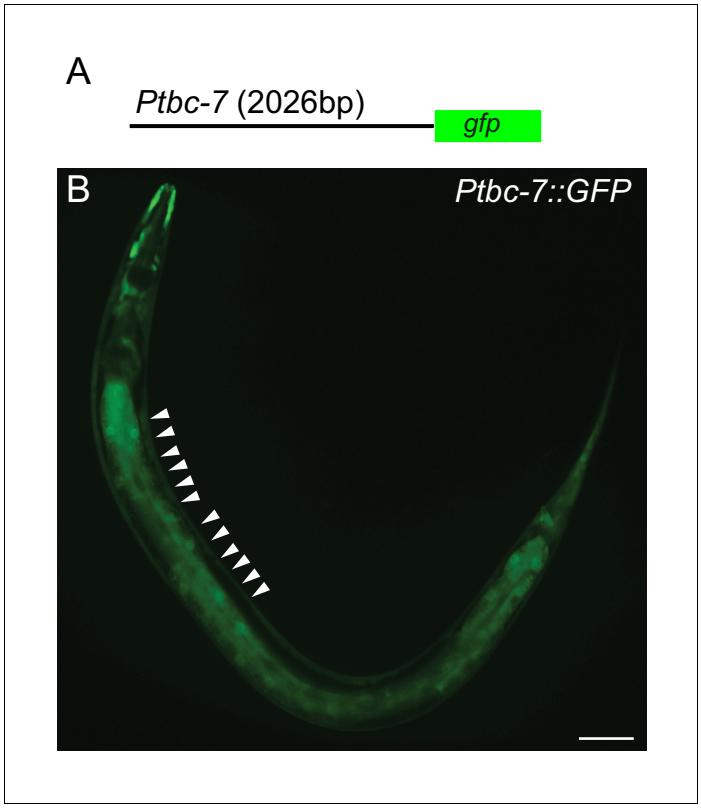

Figure 2—figure supplement 2. *tbc-7* expression pattern. (**A**) DNA construct containing a 2026 bp *tbc-7* promoter upstream of *gfp* coding sequence was used to generate an extrachromosomal array to report *tbc-7* expression. (**B**) Expression of *gfp* controlled by the *tbc-7* promoter is detected in the intestine, unidentified head cells and BWM cells (white arrowheads). Scale bar, 20 μm.

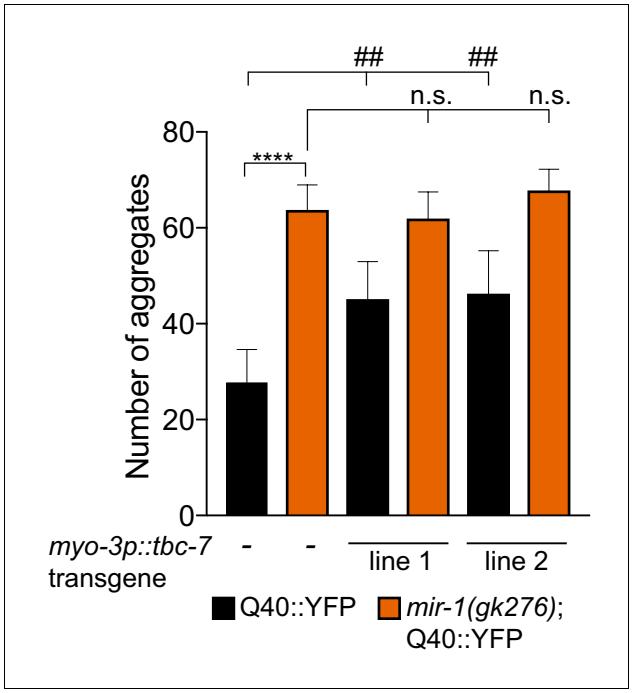

Figure 2—figure supplement 3. Overexpression of *tbc-7* causes Q40::YFP aggregation. Quantification of Q40::YFP aggregates in wild-type and *mir-1(gk276)* animals transgenically-expressing *tbc-7* cDNA in body wall muscle (*myo-3* promoter). Experiments were performed in triplicate (n = 30). Error bars show standard error of the mean (SEM). ****p<0.0001, ## p<0.001 compared to the control and n.s. not significant compared to *mir-1(gk276)* (one-way ANOVA analysis, followed by Dunnett's multiple comparison test).

Figure 2—figure supplement 4. *miR-1* targeting of TBC proteins is conserved. Predicted *mir-1* binding sites are found in the 3′UTRs of mRNAs that encode TBC proteins in *C. elegans* (*tbc-7*), *D. melanogaster* (Skywalker) and humans (TBC1D15). This conservation is found in all vertebrate species examined (Targetscan). The *mir-1* seed sequences are shown in blue and the predicted *tbc-7*-related 3′UTRs are shown in green.

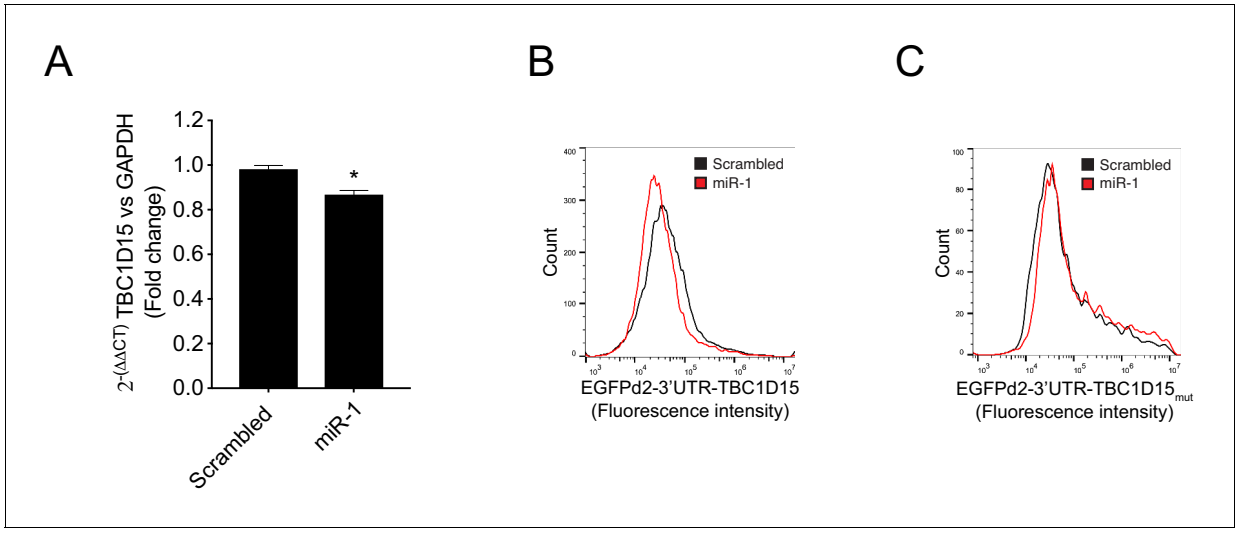

Figure 2—figure supplement 5. TBC1D15 3′UTR analysis. (**A**) Relative TBC1D15 mRNA levels normalized to GAPDH measured by qRT-PCR from HeLa cells expressing scrambled miRNA or miR-1 mimic. Bar graph show fold changes compared to scrambled control ± SEM (n = 3). (**B–C**) Representative fluorescence intensity histograms from flow cytometry analysis of HeLa cells expressing scrambled miRNA (Scr) or miR-1 mimic together with (**B**) GFPd2-3′UTR-TBC1D15 or (**C**) GFPd2-3′UTR-TBC1D15 containing mutated miR-1 target sequence. Quantification of these histogram data is shown in ***Figure 2J–K***. Wild-type hsa TBC1D15 3′UTR = 5′-CUUUCCUUUUCGAUAACAUUCCU-3′ and mutated hsa TBC1D15 3′UTR = 5′-CUUUCCUUUUCGA UAAAAUUACU-3′.

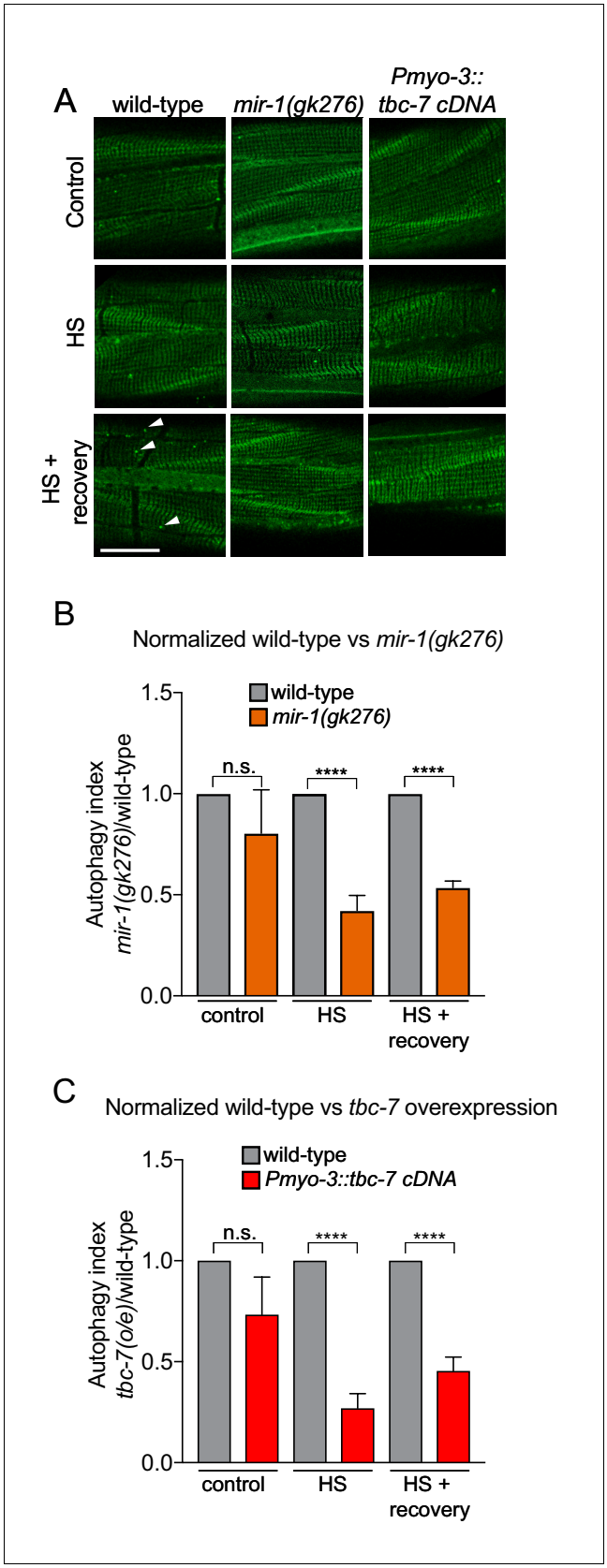

Figure 3. *mir-1* and *tbc-7* control stress-induced autophagy. (**A**) Fluorescent images of BWM expressing GFP::LGG-1/Atg8 in wild-type, *mir-1(gk276)* and *Pmyo-3::tbc-7* overexpressing animals under control conditions,

Figure 3 continued on next page

Figure 3 continued

immediately after heat shock for 1 hr at 35°C (HS) or 1 hr after recovery from heat shock at 15°C (HS + recovery). GFP::LGG-1 puncta = arrowheads. Scale bar, 10 µm. (**B–C**) Quantification of GFP::LGG-1/Atg8 puncta in BWM of animals and conditions shown in (**A**). The values represent the number of green puncta in *mir-1(gk276)* (**B**) and *Pmyo-3::tbc-7* overexpressing (**C**) animals normalized to one green puncta in wild-type animals for each condition. n > 15. ± SEM ****p<0.0001, n.s. not significant (Welch's t-test).

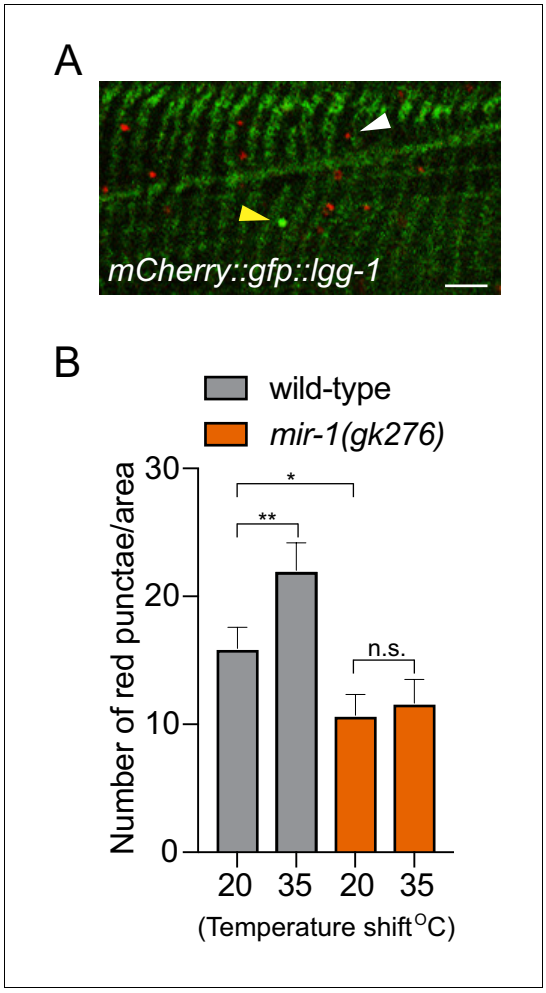

Figure 3—figure supplement 1. mir-1 controls stress-induced autophagy. (**A**) Fluorescent image of BWM expressing mCherry::GFP::LGG-1 in wild-type animals. Yellow arrowhead = autophagosome and white arrowhead = autolysosome. Scale bar, 10 μm. (**B**) Quantification of autolysosomes in BWM of wild-type and *mir-1(gk276)* animals incubated at 20°C and then shifted for 1 hr at 35°C. The values represent the mean number of red puncta (autolysosomes). n > 15. ± SEM ****p<0.0001, n.s. not significant (Welch's t-test).

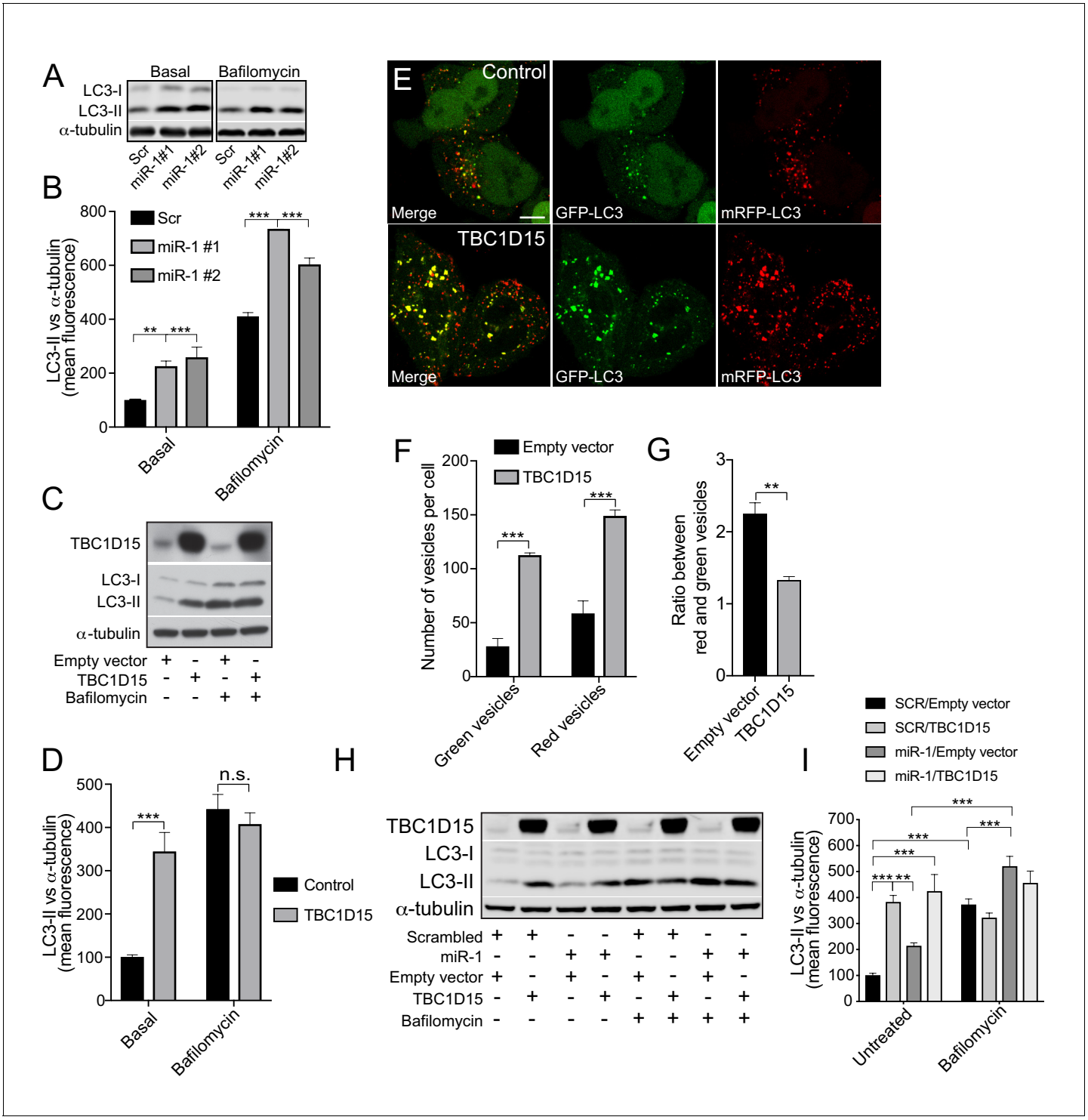

Figure 4. Human miR-1 regulates autophagy by controlling TBC1D15 expression. (**A**) WB and (**B**) quantification of LC3-II normalised to α-tubulin from HeLa cells expressing Scr or miR-1 mimics +/- bafilomycin. Data are mean fluorescence intensities of bands ± SEM (n = 3–5). **p<0.01, ***p<0.001 (one-way ANOVA with Dunnett's correction). (**C**) WB and (**D**) quantification of LC3-II normalised to α-tubulin from HeLa cells expressing empty vector (control) or TBC1D15 overexpression vector +/- bafilomycin. Data are mean fluorescence intensities of bands ± SEM normalised to α-tubulin (n = 5). n.s. not significant to the control, ***p<0.001 (two-way ANOVA with Bonferroni correction). (**E**) IF images of HeLa cells stably expressing mRFP-GFP-LC3 and transfected with empty vector (control) or TBC1D15 overexpression vector. Scale bar, 10 μm. (**F**) Quantification of green and red vesicles and (**G**) red/green vesicle ratio from (**E**) ± SEM (n = 3, 12–14 cells per replicate). **p<0.01, ***p<0.001 (Student's t-test). (**H**) WB and (**I**) quantification of HeLa cells co-transfected with Scr or miR-1 mimic together with empty vector or TBC1D15 overexpression vector +/- bafilomycin. Data are mean fluorescence intensities of LC3-II bands normalized to α-tubulin ± SEM (n = 7). **p<0.01, ***p<0.001 (two-way ANOVA with Bonferroni correction).

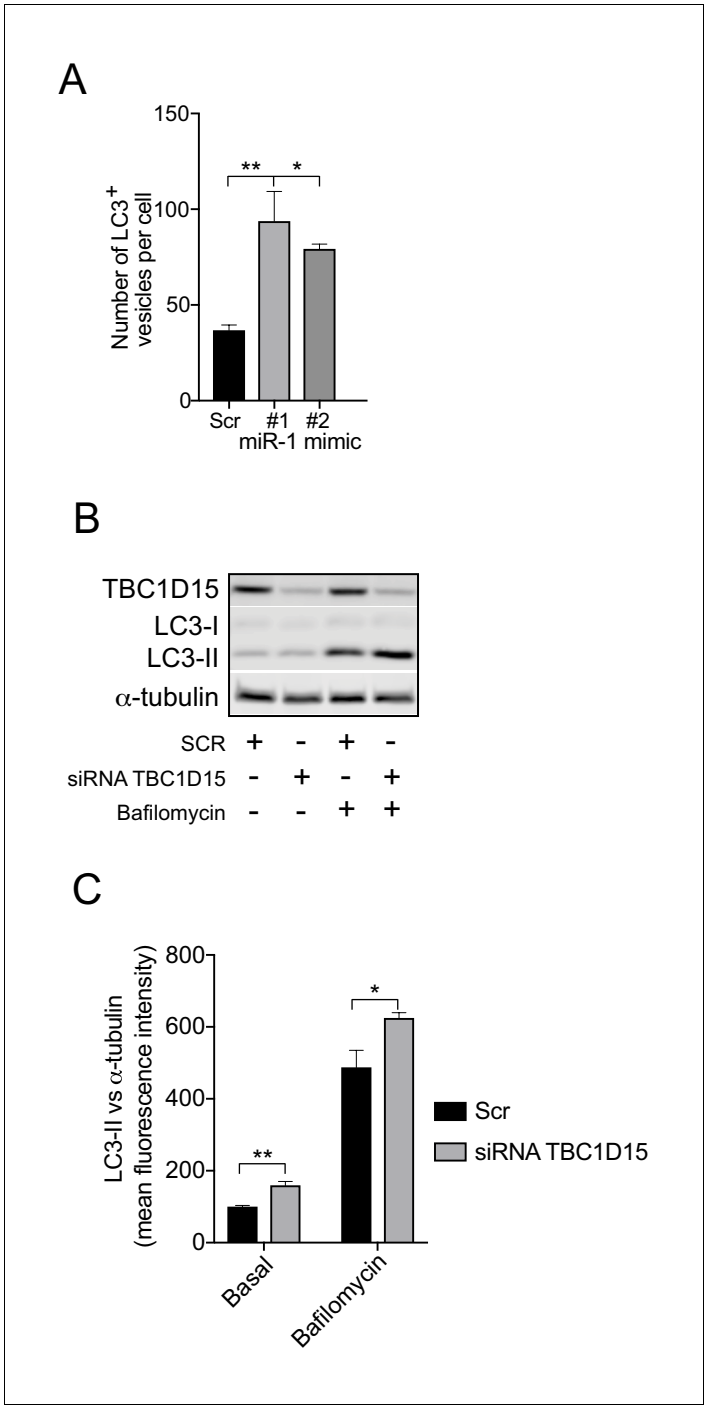

Figure 4—figure supplement 1. miR-1 and TBC1D15 control autophagy. (**A**) Quantification of the mean number of LC3-positive vesicles per HeLa cell ± SEM expressing scrambled miRNA (Scr) or independent miR-1 mimics immunostained with antibodies against LC3 (n = 3). *p<0.05, **p<0.01 (one-way ANOVA with Dunnett's correction). (**B**) WB of HeLa cells transfected with Scr siRNA or siRNA against TBC1D15 in the presence or absence of bafilomycin (400 nM for 4 hr). (**C**) Mean fluorescence intensities of LC3-II WB bands ± SEM normalized to α-tubulin (n = 4). *p<0.05, **p<0.01 (Student's t-test).

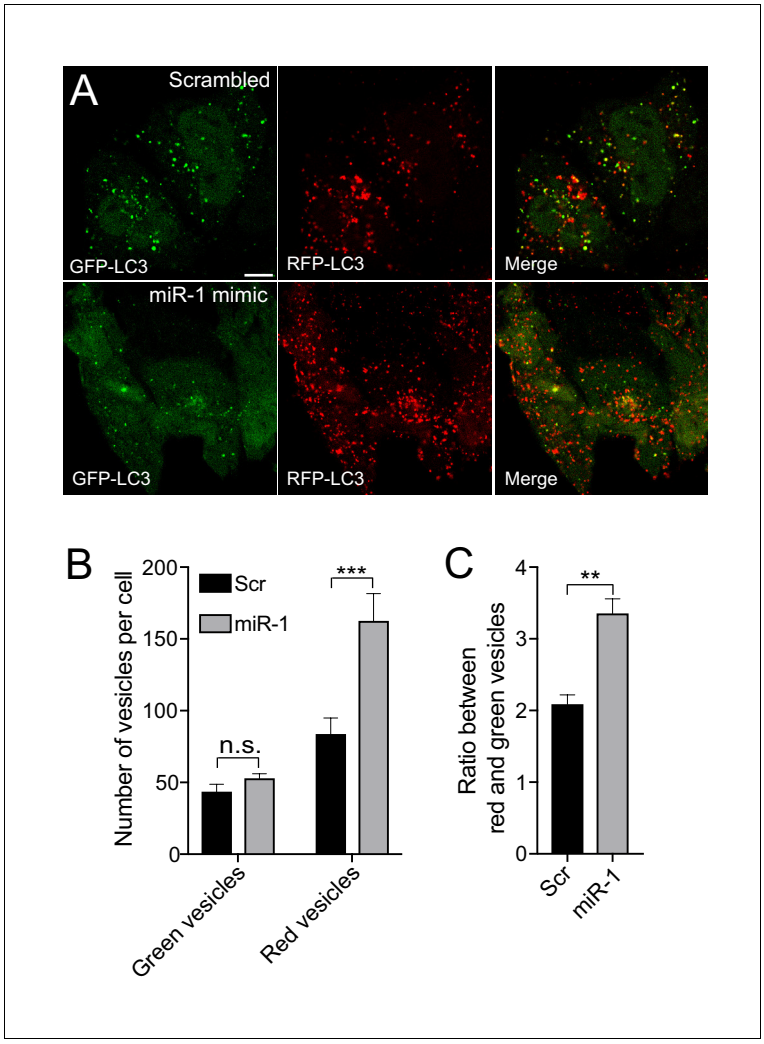

Figure 4—figure supplement 2. miR-1 overexpression induces autophagy flux. (**A**) IF images of HeLa cells stably expressing mRFP-GFP-LC3 and transfected with scrambled miRNA (Scr) or miR-1 mimic. Scale bar, 10 μm. (**B**) Quantification of mean number of green and red vesicles per cell and (**D**) the red/green vesicle ratio ± SEM (n = 4). **p<0.01, ***p<0.001 (Student's t-test).

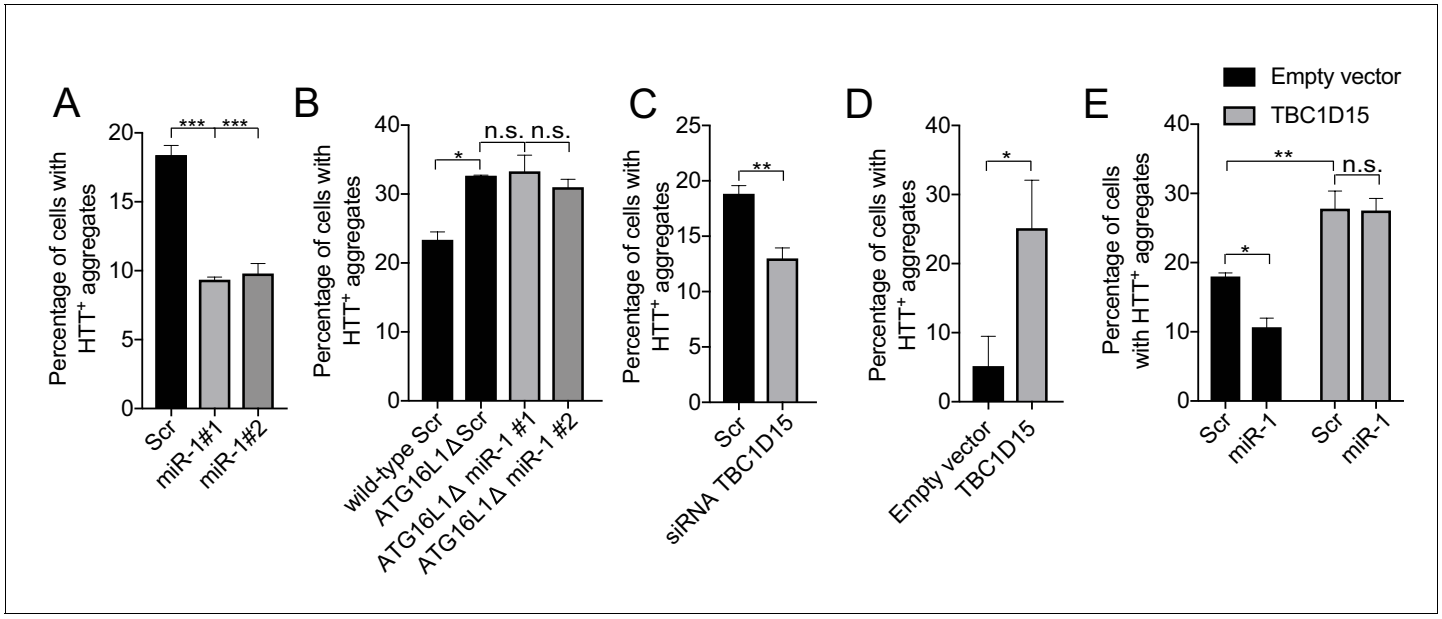

Figure 5. miR-1 reduces mutant Huntingtin aggregation through the autophagy pathway. (**A**) Quantification of the percentage of cells containing HTT-positive aggregates co-expressing scrambled (Scr) or miR-1 mimics with EGFP-HTT_{Q74} for 48 hr ± SEM (n = 3, 200–400 cells per replicate). ***p<0.001 (one-way ANOVA). (**B**) CRISPR/Cas9 ATG16L1 knockout HeLa cells co-expressing scrambled (Scr) or miR-1 mimics with EGFP-HTT_{Q74} for 48 hr. Quantification of the percentage of cells containing HTT-positive aggregates ± SEM (n = 3, 200–400 cells per replicate). *p<0.05 (Student's t-test), n.s. not significant (one-way ANOVA). (**C–E**) Quantification of the percentage of cells containing HTT-positive aggregates in HeLa cells co-expressing EGFP-HTT_{Q74} with (**C**) scrambled (Scr) or siRNA against TBC1D15 for 48 hr (n = 4, 200–400 cells per replicate), (**D**) empty or TBC1D15 overexpression vector for 24 hr (n = 3, 200–400 cells per replicate), or (**E**) a combination of Scr or miR-1 mimic together with empty or TBC1D15 overexpression vector for 48 hr (n = 6, 200–400 cells per replicate) ± SEM. (**C–D**) *p<0.05, **p<0.005, n.s. not significant (Student's t-test) or (**E**) (two-way ANOVA with Dunnett's correction).

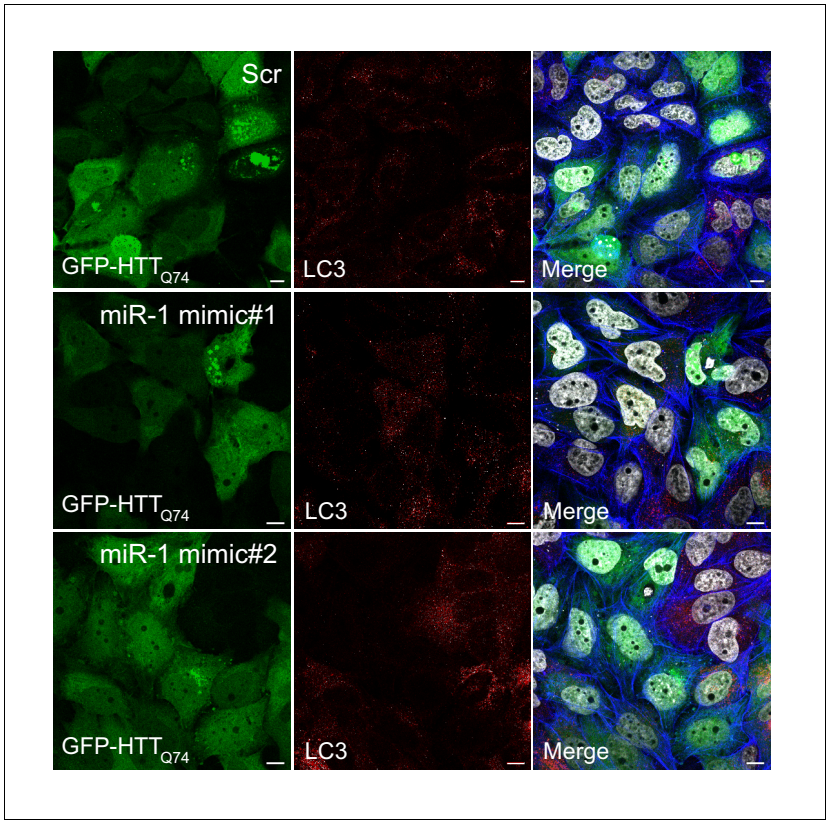

Figure 5—figure supplement 1. miR-1 overexpression reduces HTT_{Q74} accumulation IF images of HeLa cells co-expressing scrambled miRNA (Scr) or independent miR-1 mimics with EGFP-HTT_{Q74} stained with antibodies against LC3 (red), phalloidin (blue), and DAPI (gray). Scale bar, 10 μm.

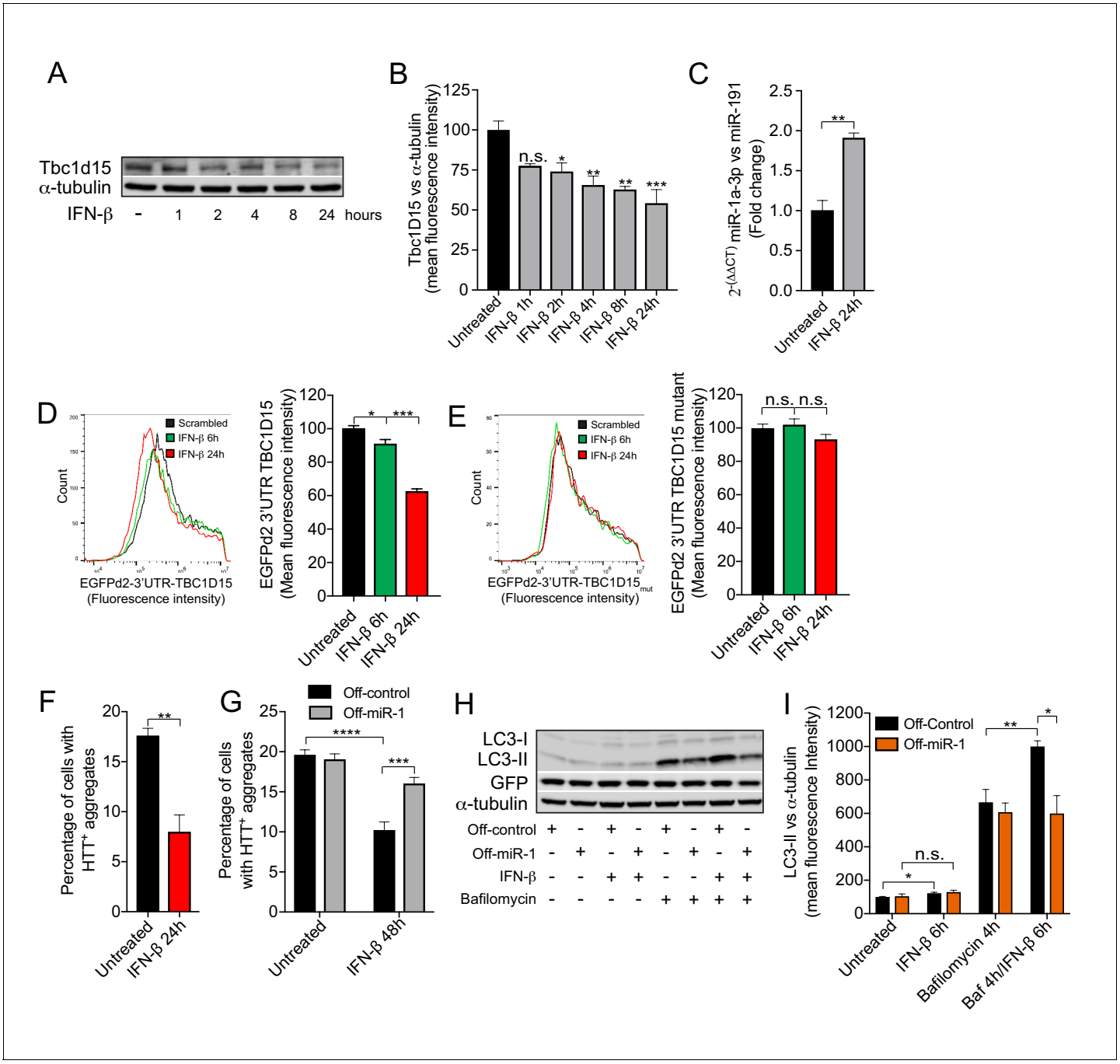

Figure 6. IFN-β induction of miR-1 controls mutant Huntingtin aggregation. (**A**) WB and (**B**) quantification of Tbc1d15 normalized to α-tubulin of cortical neurons from mice treated with recombinant mouse IFN-β (100 U/ml) for 1–24 hr (n = 4). Data are mean fluorescence intensities of bands ± SEM. n.s. not significant to the control, *p<0.05, **p<0.01, ***p<0.001 (one-way ANOVA). (**C**) RT-PCR of miR-1a-3p normalized to miR-191 from mouse cortical neurons treated with recombinant mouse IFN-β (100 U/ml) for 24 hr (n = 3). **p<0.01 (Student's t-test). (**D–E**) Flow cytometry analysis of HeLa cells expressing (**D**) GFPd2-3'UTR TBC1D15 (n = 4) or (**E**) mutated GFPd2-3'UTR TBC1D15$_{mutant}$ (n = 5) treated with recombinant human IFN-β (1000 U/ml) for 6 or 24 hr. Data are presented as fluorescence intensity histograms and bar graphs showing mean fluorescence intensities ± SEM. *p<0.05, ***p<0.0001 (one-way ANOVA). (**F**) Quantification of HTT$_{Q74}$ aggregates in HeLa cells expressing EGFP-HTT$_{Q74}$ treated with recombinant human IFN-β (1000 U/ml) for 24 hr. Graph shows percentage of cells containing EGFP-HTT$_{Q74}$-positive aggregates (n = 4, 400 cells per replicate) ± SEM. **p<0.01 (Student's t-test). (**G**) Quantification of HTT$_{Q74}$ aggregates in HeLa cells expressing GFP-Off-control or GFP-Off-miR-1 (miR-1 hairpin inhibitor) with EGFP-HTT$_{Q74}$ and treated with recombinant human IFN-β (1000 U/ml) for 48 hr. Graph represents percentage of cells containing EGFP-HTT$_{Q74}$-positive aggregates (n = 5, 400 cells per replicate) ± SEM. ***p<0.001, ****p<0.0001 (two-way ANOVA with Bonferroni correction). (**H**) WB of LC3, GFP and α-tubulin and (**I**) quantification of LC3-II normalized to α-tubulin from HeLa cells stably expressing GFP-Off-Control and GFP-Off-miR-1 treated with

Figure 6 continued on next page

Figure 6 continued

recombinant human IFN-β (1000 U/ml) for 6 hr, bafilomycin (400 mM) for 4 hr or in combination (n = 4) ± SEM. *p<0.05, **p<0.01, n.s. not significant (Student's t-test).

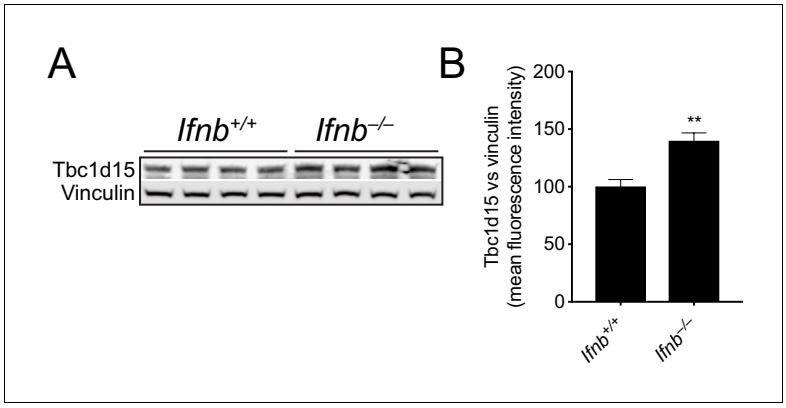

Figure 6—figure supplement 1. IFN-β regulates TBC1D15 expression the mouse brain. (**A**) WB and (**B**) quantification of Tbc1d15 (normalized to vinculin) in the brain of wild-type (*Ifnb*$^{+/+}$) and *Ifnb*$^{-/-}$ 3 month old male mice (n = 4). Data are mean fluorescence intensities of bands ± SEM. **p<0.01 (Student's t-test).

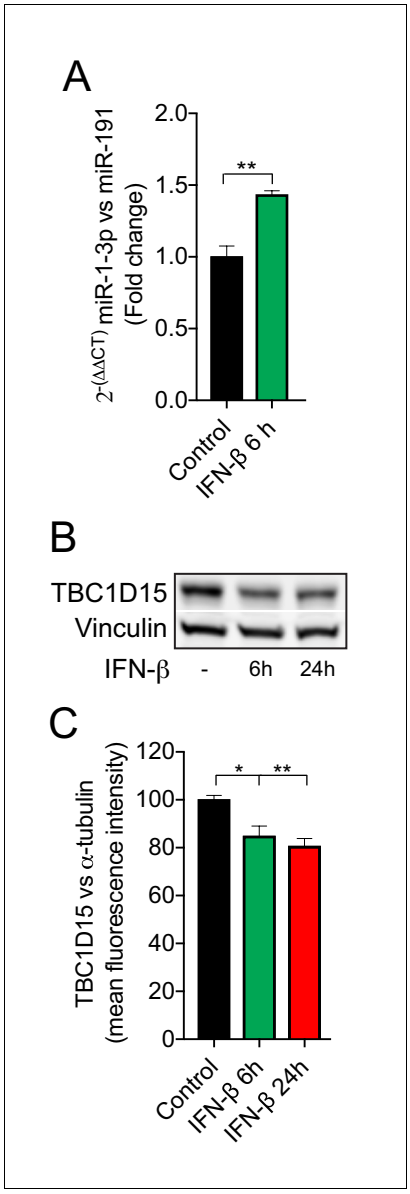

Figure 6—figure supplement 2. IFN-β regulates miR-1 and TBC1D15 expression in HeLa cells. (**A**) RT-PCR of miR-1–3 p normalized to miR-191 from HeLa cells treated with recombinant human IFN-β (1000 U/ml) for 6 hr (n = 3). **p<0.01 (Student's t-test). (**B**) WB and (**C**) quantification of TBC1D15 bands normalised to vinculin from HeLa cells treated with recombinant human IFN-β for 6 or 24 hr (n = 4). Data are mean fluorescence intensities ± SEM. *p<0.05, **p<0.01 (one-way ANOVA).

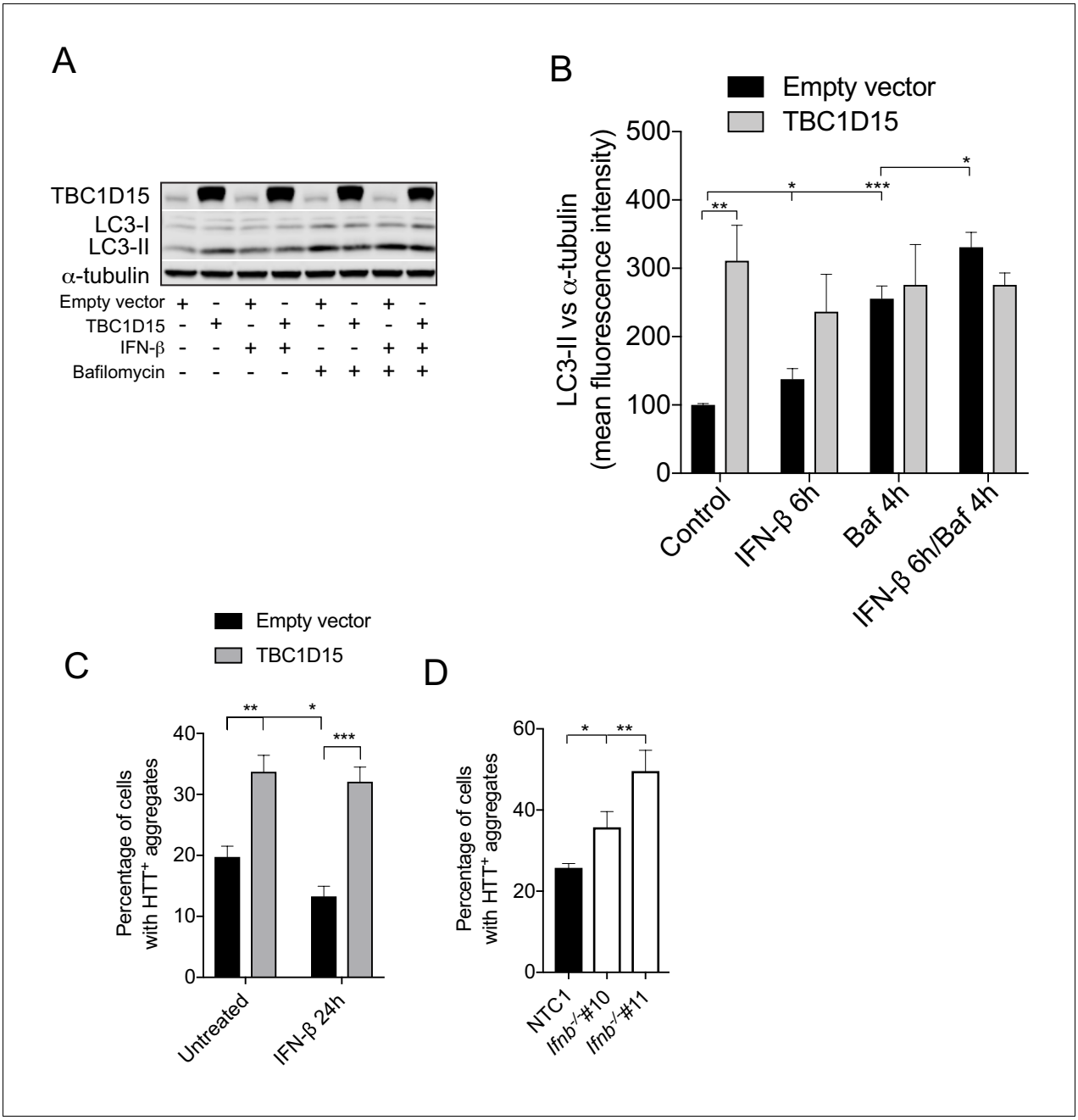

Figure 6—figure supplement 3. TBC1D15 overexpression abrogates IFN-β-induced reduction of HTT_{Q74} aggregates. (**A**) WB of TBC1D15, LC3 and α-tubulin in HeLa cells expressing empty or TBC1D15 overexpression vector, treated with recombinant human IFN-β (1000 U/ml) for 6 hr, bafilomycin (400 mM) for 4 hr, or a combination of both. (**B**) Quantification of mean fluorescence intensities of LC3-II bands from (**A**) (n = 4) ± SEM. *p<0.05, **p<0.01 ***p<0.001 (Student's t-test). (**C**) HeLa cells co-expressing EGFP-HTT_{Q74} with either empty or TBC1D15 overexpression vector with or without recombinant human IFN-β treatment (1000 U/ml) for 24 hr. Graph represents percentage of cells containing EGFP-HTT_{Q74}-positive aggregates ± SEM. *p<0.05, **p<0.01 ***p<0.001 (Student's t-test). (**D**) Neuronally differentiated N2A cells with non-targeting control-1 (NTC1) or *Ifnb* CRISPR/Cas9 knockout co-expressing EGFP-HTT_{Q74}. Graph represents percentage of cells containing EGFP-HTT_{Q74}-positive aggregates (n = 3) ± SEM. *p<0.01, **p<0.001 (Student's t-test).

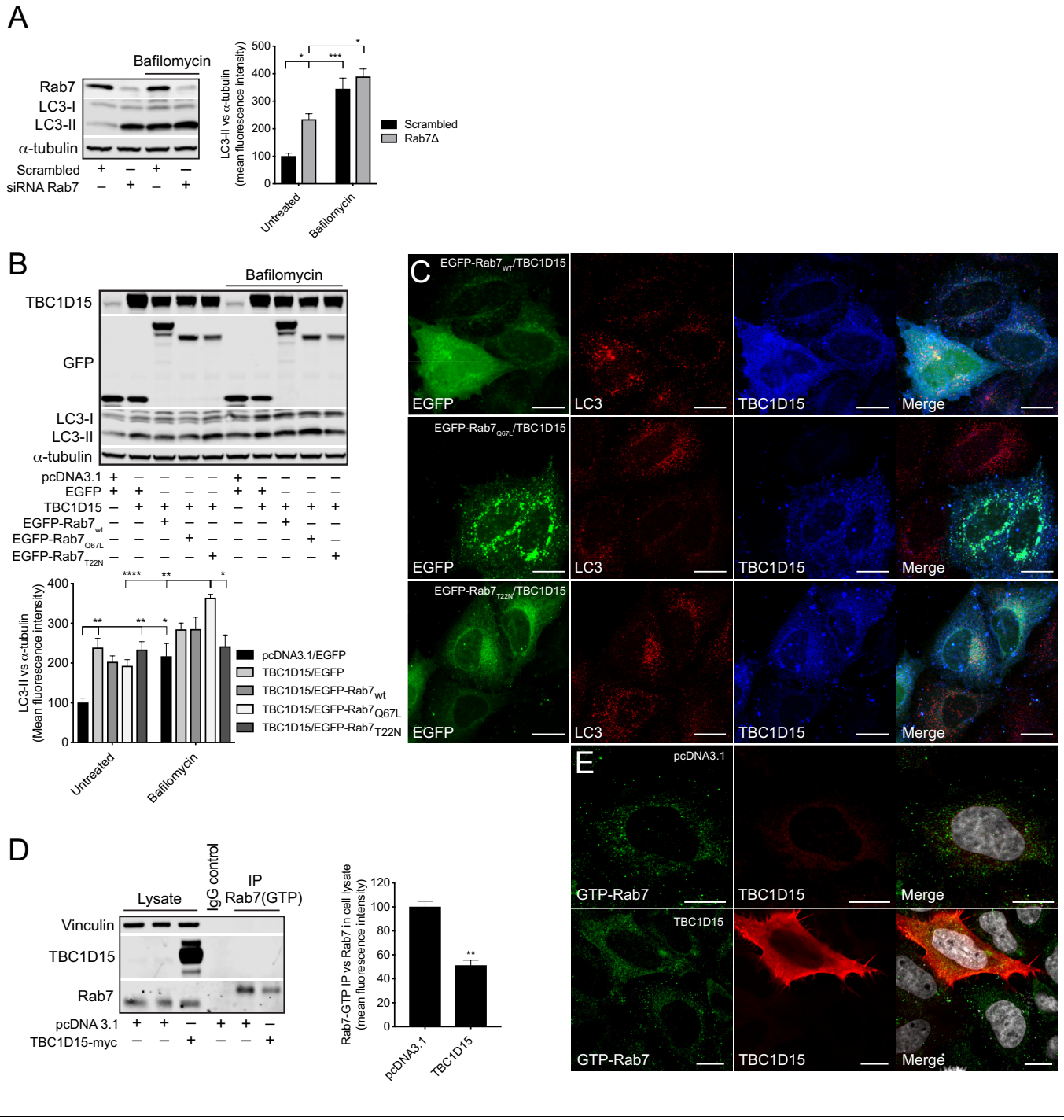

Figure 7. TBC1D15 reduces GTP-bound Rab7. (**A**) WB and quantification of LC3-II from HeLa cells transfected with scrambled siRNA or siRNA against Rab7 (Rab7Δ) +/- bafilomycin (4 hr, 400 nM). Data are mean fluorescence intensities of bands ± SEM normalised to α-tubulin (n = 3). *p<0.05, ***p<0.001 (two-way ANOVA). (**B**) WB and quantification of LC3-II normalised to α-tubulin from HeLa cells co-expressing pcDNA3.1 and EGFP, or TBC1D15 with either EGFP, pIRESneo-myc–Rab7$_{wt}$, EGFP-Rab7$_{Q67L}$, or EGFP-Rab7$_{T22N}$ for 24 hr before treatment with bafilomycin (4 hr, 400 nM). Data are mean fluorescence intensities of bands ± SEM normalised to α-tubulin (n = 6). *p<0.05, **p<0.01, ***p<0.001 (two-way ANOVA). (**C**) Immunofluorescence (IF) images of HeLa cells co-expressing TBC1D15 with pIRESneo-myc-Rab7$_{wt}$, EGFP-Rab7$_{Q67L}$ or EGFP-Rab7$_{T22N}$ stained with antibodies against LC3 and TBC1D15. Scale bars, 10 μm. (**D**) WB showing immunoprecipitation (IP) of GTP-bound (active) Rab7 from HeLa expressing pcDNA3.1 or TBC1D15. Data are mean fluorescence intensities of GTP-bound Rab7 (IP) normalized to the endogenous level of Rab7 (cell lysate) ± SEM

Figure 7 continued on next page

Figure 7 continued

(n = 3). **p<0.01 (Student's t-test). (E)IF of HeLa cells expressing empty vector or TBC1D15 stained with antibodies against GTP-bound Rab7, TBC1D15 and DAPI. Scale bar, 10 μm.